ACS APPLIED MATERIALS & INTERFACES

Research Article

www.acsami.org

Facile Method To Disperse Nonporous Metal Organic Frameworks: Composite Formation with a Porous Metal Organic Framework and Application in Adsorptive Desulfurization

Zubair Hasan[†] and Sung Hwa Jhung*

Department of Chemistry and Green-Nano Materials Research Center, Kyungpook National University, Daegu 702-701, Republic of Korea

Supporting Information

ABSTRACT: It is generally not easy to utilize nonporous metal organic frameworks (MOFs) with a large crystal size (especially for catalysis or adsorption) because their surface area is low and the majority of the active sites exist inside the MOFs. Composing with porous materials may be one way to disperse the nonporous materials. In this study, a nonporous/nonsoluble MOF (in which the particle size was much larger than the cavity size of the porous MOFs) containing Cu(I) ($(Cu_2(pyz)_2(SO_4)(H_2O)_2)_n$, denoted as CP) was composed with typical porous MOFs such as MIL100-(Fe) (iron-benzenetricarboxylate) and CuBTC (cupper-benzene-tricarboxylate). The Cu(I) species of the nonporous MOF was effectively utilized for the adsorptive desulfurization (ADS) of model fuel. Even though the porosities of the composed MOFs decreased as the content of CP increased, the adsorption capacity increased as the content of CP increased (up to a certain content). Considering the negligible capacity of CP for ADS, the enhanced adsorption capacity may be a result of the well-dispersed Cu(I), which is known to be beneficial for ADS via π-complexation. The dispersed CP was also observed by transmission electron microscopy mapping. Therefore, composing a nonporous MOF with porous MOF is a new and facile way to disperse/utilize the active sites of a nonporous MOF.

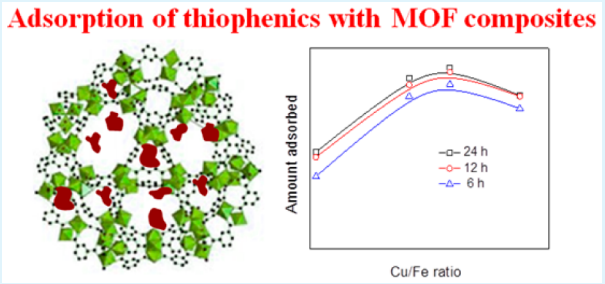

KEYWORDS: *adsorption, adsorptive desulfurization, composites, metal organic frameworks, π-complexation*

1. INTRODUCTION

Recently, considerable progress has been made in the field of nanoporous materials as a result of newly developed advanced functional materials[1−5] including metal organic frameworks (MOFs).[6−14] MOF-type materials are important because of their remarkable porosity, facile tunability of their pore shape/size (not only microporous structure but also mesoporous one), and their potential applications which include adsorption/storage[8,13] and separation.[9,10,12] The application of MOFs for the adsorptive removal of hazardous contaminants from both liquid and vapor phases have also recently been studied.[7,11,15−17] It was revealed that virgin MOFs possess potential physicochemical properties which could be advantageous for different applications. However, their properties can be further enhanced by tuning the structure or chemical nature by using several methods. Some popular methods include the grafting or postsynthetic modification of functionalized groups,[18] using functionalized organic linkers,[19,20] impregnation of appropriate active species,[21,22] and producing MOF composites with suitable materials.[23,24] MOF composites are a comparatively new concept and have already drawn significant scientific interest as their successful synthesis can entirely alter their physicochemical properties[23,24] as well as improving their range of potential applications.[25−27]

So far, various materials have been used to prepare MOF composites. Examples include polyoxometalates (POM),[28] iron oxide,[29] silica,[30] graphite oxide (GO),[31] carbon nanotubes,[32] and graphene oxide.[33] There are several methods used to prepare MOF composites and one of these methods is called bottle-around-ship (BAS).[34] During this method, presynthesized composing materials are added to the MOF precursors to continue the synthesis procedure. For example, composing materials of GO or Fe_3O_4 (with a small size) have been added to the MOF precursors to prepare GO/MOF[24,31] or Fe_3O_4/HKUST-1.[35] To prepare MOF composites via BAS, the size of the composing materials should be small in comparison to the cavity size of the porous material. Iron oxide/MOF composites are interesting because of the magnetic separation of the composite materials. GO/MOF composites are also interesting because of their improved porosity; therefore, these composites have been used in various adsorptions.[24,31] In similar methods, soluble composing materials (such as POM) are mixed with the MOF precursors, and following the completion of the synthesis procedure, the MOFs are formed, trapping the composing

Received: February 21, 2015
Accepted: April 27, 2015
Published: April 27, 2015

DOI: 10.1021/acsami.5b01642
ACS Appl. Mater. Interfaces 2015, 7, 10429−10435

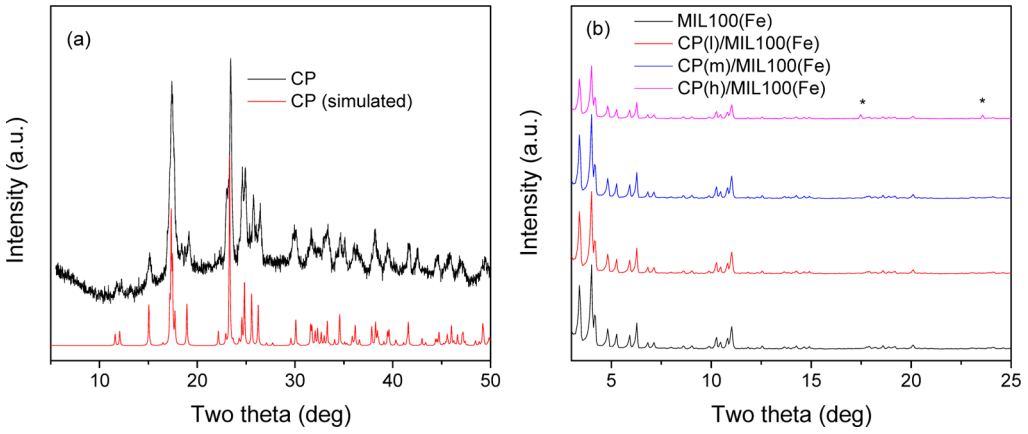

Figure 1. XRD patterns of (a) CP and simulated CP; (b) MIL100(Fe) and CP/MIL100(Fe) composites. * represents the diffractions from CP.

materials.[36] POM/MOF composites have been used in various fields including acid catalysis, oxidation catalysis, and adsorption/decontamination.[37,38] However, so far, there are no reports on the preparation of MOF composites which have both porous MOF and nonporous MOF, especially with a large crystal size.

Recently, it is important to remove sulfur-containing compounds (SCCs) (including benzothiophene (BT), dibenzothiophene (DBT), and dimethyldibenzothiophenes) from commercial fuels to prevent air pollution and catalysts deactivation. According to United States and European Union regulations, the acceptable sulfur contents in commercial fuels are limited to 15 and 10 μg/g, respectively.[39,40] Up to now, a variety of methods including hydrogenation, adsorption, and oxidation have been tried for sulfur removal.[39−41] Adsorptive purification might be one of the most competitive methods to reduce sulfur content up to ultralow values.[40] Cu(I)-containing materials have been effectively used for adsorptive desulfurization because of their ability to form π-complexation with SCCs.[42,43] Yang et al. prepared Cu(I)-containing zeolitic adsorbents via ion exchange which requires high-temperature calcination.[42] On the other hand, Cu(I)-containing porous materials such as MCM-41, SBA-15, and Al_2O_3 have also been prepared through the loading of Cu_2O. During these cases, copper salts were initially impregnated onto a porous support; subsequently, calcination (in the presence of air) was conducted to form CuO. Finally, Cu_2O was formed through high-temperature calcination under inert conditions.[44,45] Well-dispersed Cu(I) materials over porous solids can enhance the overall adsorption of SCCs; however, the main difficulty in using MOF as a porous support is due to its low thermal stability. Therefore, it is important to develop some alternative ways to disperse the Cu(I) onto thermally unstable porous supports without applying calcination at high temperature. So far, only a few studies have been conducted to prepare Cu(I) materials dispersed onto MOFs such as Cu(I)/vanadium-benzenedicarboxylate, Cu(I)/iron-benzenetricarboxylate, or Cu(I)/iron-benzenetricarboxylate[46−48] at low temperature. However, this particular field requires further investigation.

The synthesis and stabilization of Cu(I)-containing materials are difficult because of the intrinsic instability of the Cu(I) state and the facile oxidation to Cu(II).[49,50] However, stable Cu(I) compounds have recently been synthesized using pyrazine-based linkers.[50] Additionally, in comparison to Cu(II), there are scarce reports on Cu(I)-containing MOFs or coordination polymers (COP).[50−53] Moreover, among the reported Cu(I)-containing MOFs/COPs, only a few have demonstrated permanent porosity.[50,51] Porosity is an important and vital property of MOFs which is required to extend its potentials mainly for adsorption and catalysis. To take advantage of the Cu(I) species, one method may involve the dispersion of the nonporous Cu(I)-containing materials onto highly porous MOFs.

In this study, we demonstrate a new attempt to prepare MOF composites via the dispersion of nonporous/nonsoluble Cu(I)-containing species (the size is much larger than that of cavities of the porous MOFs) to another MOF. Among the many MOFs which have been reported so far, two widely studied MOFs, iron-benzenetricarboxylate $[Fe^{(III)}{}_3O(H_2O)_2(F)\{C_6H_3(CO_2)_3\}_2{\cdot}nH_2O$ ($n \sim 14.5$),[54] denoted as MIL100(Fe)] and copper-benzenetricarboxylate $[Cu_3\{C_6H_3(CO_2)_3\}_2(H_2O)_3$; denoted as CuBTC],[55] have been used in this study. Both MIL100(Fe) and CuBTC have been investigated for their adsorption properties.[35,47] A stable nonporous Cu(I)-containing compound ($((Cu_2(pyz)_2(SO_4)(H_2O)_2)_n$, denoted as CP) has been hydrothermally synthesized using $CuSO_4$ and pyrazine under microwave (MW) irradiation.[53] The CP was subsequently employed to form composites with porous MIL100(Fe) or CuBTC. The prepared CP/MIL100(Fe) or CP/CuBTC composites were applied to the adsorptive desulfurization of SCCs to utilize the well-dispersed Cu(I).

2. EXPERIMENTAL SECTION

2.1. Materials. All the solvents and reactants were commercially available and were used as received. Copper sulfate ($CuSO_4$, 99%), copper nitrate trihydrate ($Cu(NO_3)_2{\cdot}3H_2O$, 99%), and iron nitrate nonahydrate ($Fe(NO_3)_3{\cdot}9H_2O$, 99%) were purchased from Samchun Chemicals, Korea. Pyrazine ($C_4H_4N_2$, 99%), benzoic acid (99%), trimesic acid (H_3BTC, $C_9O_6H_6$, 98%), benzothiophene (98%), and dibenzothiophene (98%) were obtained from Sigma-Aldrich. Ethanol (99.5%) and *n*-octane (99%) were procured from OCI Chemical Company, Korea.

2.2. Synthesis of Composites. The CP was synthesized under microwave (MW) irradiation following a method reported in the literature.[53] Concisely, 0.5 g of pyrazine, 0.25 g of anhydrous $CuSO_4$, 0.37 g of benzoic acid, and 15 mL of H_2O were taken into a Teflon autoclave and heated at 180 °C for 6 h under MW irradiation. The resultant red-colored solid was filtered and then washed with water and ethanol.

The syntheses of MIL100(Fe) and CuBTC were done to the following reported procedures,[56,57] and the methods are shown in the

DOI: 10.1021/acsami.5b01642
ACS Appl. Mater. Interfaces 2015, 7, 10429−10435

Supporting Information. A similar procedure was adopted for the synthesis of CP/MIL100(Fe) by adding 0.01, 0.015, and 0.025 g of CP (0.35, 0.52 and 0.86 wt % with respect to the weight of the initial iron precursor, $Fe(NO_3)_3 \cdot 9H_2O$, respectively) to the MIL100(Fe) precursor. The obtained solids were denoted as CP(l)/MIL100(Fe), CP(m)/MIL100(Fe), and CP(h)/MIL100(Fe), respectively. The CP(l)/CuBTC and CP(m)/CuBTC samples were synthesized using a similar method, following the processes described above.

2.3. Characterization. The obtained adsorbents were characterized with X-ray diffraction (XRD), field-emission transmission electron microscopy/energy-dispersive spectroscopy (FE-TEM/EDS), scanning electron microscopy (SEM), X-ray photoelectron spectroscopy (XPS), and nitrogen adsorption. Detailed experimental procedures are shown in the Supporting Information.

2.4. Adsorption Experiments. Adsorption experiments were carried out to follow a method reported earlier.[47] Briefly, BT or DBT solutions in *n*-octane were used in the adsorption, and BT or DBT concentrations were determined using a gas chromatograph. Detailed experimental procedures are shown in the Supporting Information. The adsorption kinetic constants were calculated using the pseudo-second-order rate equation that was obtained by a nonlinear model (see Supporting Information). The maximum adsorption capacity (Q_0) and separation factor (R_L) were obtained using the Langmuir equation (see Supporting Information).

3. RESULTS AND DISCUSSION

3.1. Properties of the Adsorbents. The crystal structure of the obtained CP was confirmed by the correlation of the XRD patterns with the calculated one (Figure 1a). Figure 1b and Supporting Figure 1 show the XRD patterns of the MIL100(Fe), CP/MIL100(Fe), CuBTC, and CP/CuBTC composites. The XRD patterns demonstrate that the MOFs were successfully synthesized, irrespective of the introduction of CP during the synthesis. However, representative peaks of CP, even at very low intensities, were observed for CP(h)/MIL100(Fe). (The zoomed XRD patterns are shown in Supporting Figure 2.) The XPS analysis (Figure 2) was

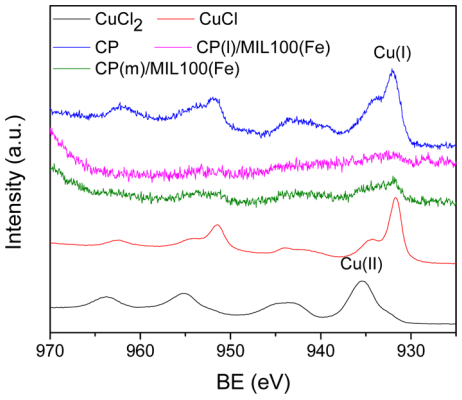

Figure 2. XPS spectra in copper region of CP and CP/MIL100(Fe) composites. The spectra of $CuCl_2$ and CuCl are also shown as references.

conducted to determine the oxidation state of Cu in the CP and CP/MIL100(Fe) composites. The XPS analyses of both pure CuCl and $CuCl_2$ were also conducted for reference. As shown in Figure 2, the binding energy corresponding to the Cu(I) oxidation state was observed in both CuCl and CP, which ultimately confirmed the existence of Cu(I) in CP. Therefore, following the formation of the composites, the existence of Cu(I) was also observed in CP(l)/MIL100(Fe) and CP(m)/MIL100(Fe). The Cu/Fe ratios (based on wt/wt) of the obtained adsorbents were 0.016, 0.023, and 0.035 for the CP(l)/MIL100(Fe), CP(m)/MIL100(Fe), and CP(h)/MIL100(Fe), respectively (Table 1). Even though the EDS (see Supporting Figure 3) and XPS results show the existence of the copper species, no XRD peaks corresponding to the CP was observed for the CP(l)/MIL100(Fe) and CP(m)/MIL100(Fe) composites. This may be owed to the well-dispersed CP particles on the MIL100(Fe) with high porosity, which was also observed from the EDS mapping (Supporting Figure 3) of the Cu that existed in the CP. Moreover, the EDS mapping of nitrogen (which is another component of CP) also clearly confirms the sufficient dispersion of CP onto the MIL100(Fe). Therefore, it may be presumed that during the composite formation, the added presynthesized CP particles (whose size is much larger than the pore size of MIL100(Fe), as shown in Supporting Figure 4) may be in a state of dynamic equilibrium (between the large and small particles, similar to the process of Ostwald ripening) within the MIL100(Fe) precursors. Finally, following the completion of the reaction, the porous MIL100(Fe) was formed with a portion of small CP particles within the cavities. Scheme 1 shows a plausible formation mechanism of the CP/MIL100(Fe) composite with well-dispersed CP within MIL100(Fe).

Figure 3a,b shows the nitrogen adsorption isotherms and pore size distributions (PSDs) for the MIL100(Fe) and CP/MIL100(Fe) composites synthesized with various amounts of CP. The BET surface areas of CP, MIL100(Fe), and CP/MIL100(Fe) composites are shown in Table 1. Even though the surface area decreases, the shapes of the nitrogen adsorption isotherms do not noticeably change as the CP content of the CP/MIL100(Fe) composites increases. This result reveals that the decrease in the surface area with the copper content may be due to the partial blocking of the porous structure of MIL100(Fe) with the nonporous CP (which was applied for the preparation of the composites). However, even after the composite formation, the surface areas of the CP/MIL100(Fe)s are appreciable, suggesting the composites could possibly be applied in adsorption and catalysis.

3.2. Adsorption Results. Figure 4a illustrates the amounts of adsorbed BT over the CP, virgin MIL100(Fe), and CP/MIL100 (Fe) composites. All the composites exhibited higher adsorption capacities in comparison to the virgin MIL100(Fe). Although the CP itself shows negligible BT adsorption, the adsorption capacity increases significantly while composing with porous MIL100(Fe). According to Table 1, however, the pseudo-second-order rate constant (k_2) decreases in the order of MIL100(Fe) > CP(l)/MIL100(Fe) ≥ CP(m)/MIL100(Fe) > CP(h)/MIL100(Fe). This may be a result of pore blocking, which was also agreeable with Figure 3b, where a decline in the PSDs was observed with the increase of the CP contents in the CP/MIL100(Fe) composites. Importantly, from Figure 4b, it is clearly observed that the adsorption capacity of BT increases as the content of CP increases, up to a certain content, and the highest adsorbed amount of BT was observed in CP(m)/MIL100(Fe). Although the highest CP content was observed in CP(h)/MIL100(Fe), the adsorption capacity for BT was low (compared with other CP/MIL100(Fe)s). This may be as a result of an excessive degree of pore blocking due to the CP. Consequently, the CP content did not increase much during the preparation of the composites, and further studies were only conducted with the pristine MIL100(Fe) and CP(m)/MIL100(Fe).

DOI: 10.1021/acsami.5b01642
ACS Appl. Mater. Interfaces 2015, 7, 10429−10435

Table 1. Physiochemical Properties and the Results for the BT Adsorption over MIL100(Fe) and CP/MIL100(Fe) Composites

adsorbents	BET surface area (m^2/g)	total pore volume (cm^3/g)	Cu/Fe ratio[a]	Q_0 (mg/g)	b[c] (L/mg)	r^2 (Langmuir plot)	k_2 (nonlinear) (g/mg·h)[d]	r^2 (nonlinear kinetics)
CP	29	0.01		ND[e]	ND[e]	ND[e]	ND[e]	ND[e]
MIL100(Fe)	1650	0.79		114(69.1)	1.65×10^3	0.998	0.013	0.999
CP(l)/MIL100(Fe)	1399	0.71	0.016	ND[e]	ND[e]	ND[e]	0.011	0.999
CP(m)/MIL100(Fe)	1328	0.67	0.023	128 (96.4)	2.43×10^3	0.999	0.011	0.998
CP(h)/MIL100(Fe)	1204	0.61	0.035	ND[e]	ND[e]	ND[e]	0.009	0.999

[a]wt/wt ratio, calculated from EDS (TEM). [b]Value in the parentheses: adsorption capacity of BT per unit surface area (square meter) of adsorbents ($\mu g/m^2$). [c]Langmuir constant. [d]At 1000 μg/g of BT. [e]Not determined.

Scheme 1. Schematic Representation of the Formation of CP/MIL100(Fe) Composite

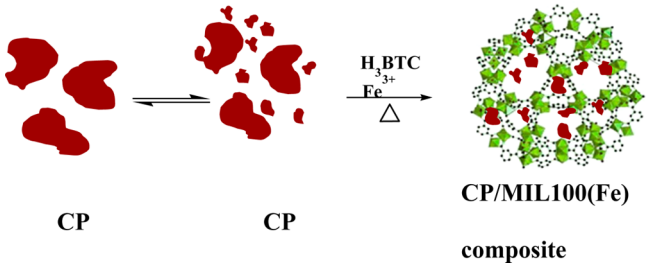

The adsorption isotherms of the MIL100(Fe) and CP(m)/MIL100(Fe) were obtained after adsorption for 24 h, and the results are summarized in Figure 5a. Langmuir plot (Figure 5b) was used to calculate the maximum adsorption capacities (Q_0); the Q_0 values are summarized in Table 1. The Q_0 values for the MIL100(Fe) and CP/MIL100(Fe) were 114 and 128 mg/g, respectively. This demonstrates an increase of 12.3% for the maximum adsorption capacity of the CP(m)/MIL100 (Fe) (even with low porosity) when compared with the pristine MIL100(Fe). More importantly, the Q_0 value based on surface area (adsorption capacity per square meter of adsorbents, $\mu g/m^2$) increased by 39.5% upon composing (from 69.1 to 96.4 $\mu g/m^2$ for MIL100(Fe) and CP(m)/MIL100(Fe), respectively). Moreover, the b values also increased noticeably upon the loading of CP onto MIL100(Fe) (b(MIL100(Fe)): 1.65×10^3; b(CP(m)/MIL100 (Fe): 2.43×10^3 L/mg). As the b value is directly related to the equilibrium of adsorption,[58] the high b value obtained for CP(m)/MIL100(Fe) suggests the favorable and efficient adsorption of BT. From Supporting Figure 5, it was observed that the R_L value for CP(m)/MIL100(Fe) was lower than that for MIL100(Fe). This again shows that the adsorption over the composite was more favorable than that over MIL100(Fe) since the lower R_L value means more favorable adsorption.[59−61]

The adsorption of DBT (Figure 6) was also conducted over CP, MIL100(Fe), and CP(m)/MIL100(Fe), and high adsorption capacity was also observed for the CP(m)/MIL100(Fe). Moreover, when compared to the virgin CuBTC, a considerable enhancement in the BT adsorption was also observed for CP(m)/CuBTC (Supporting Figure 6). On the basis of the above circumstances, it is clear that a specific favorable interaction exists between BT or DBT and the Cu(I) of the CP located in the adsorbents.

As an active Cu(I) compound, Cu_2O or CuCl has been reported to demonstrate the preferential adsorption of SCCs or olefinics via π-complexation when introduced into porous supports such as zeolites, activated carbon, and MOFs.[42,43,46−48,62−68] In this study, stable nonporous CP (having Cu(I) active sites) with a larger size than the cavity of MOFs was used to prepare a well-dispersed composite with MIL100(Fe) or CuBTC and the composite accordingly demonstrated higher adsorptions of BT and DBT. This may be owed to the presence of the active Cu(I) species (in well-dispersed form) which underwent π-complexation with BT and DBT.

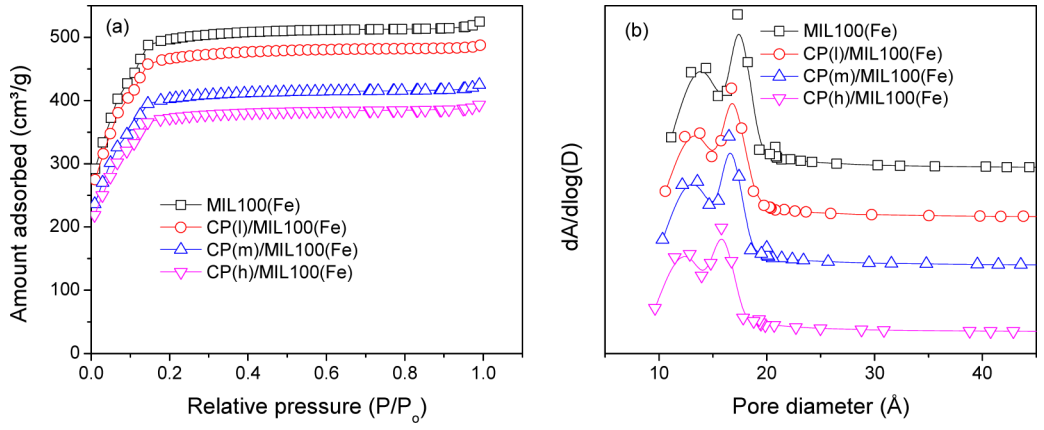

Figure 3. (a) Nitrogen adsorption isotherms and (b) Barrett−Joyner−Halenda pore size distributions of the MIL100(Fe) and CP/MIL100(Fe) composites.

DOI: 10.1021/acsami.5b01642
ACS Appl. Mater. Interfaces 2015, 7, 10429−10435

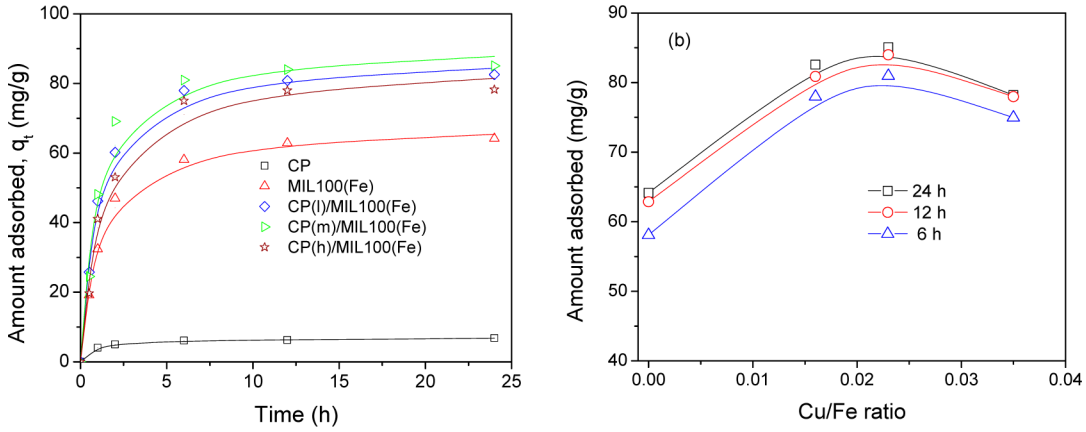

Figure 4. (a)Effect of contact time on the adsorption of BT over the CP, MIL100(Fe), and CP/MIL100(Fe)s. The solid lines show the calculated results by using pseudo-second-order nonlinear method. (b) Effect of Cu/Fe ratio of CP/MIL100(Fe) composites on the adsorption of BT at three adsorption times.

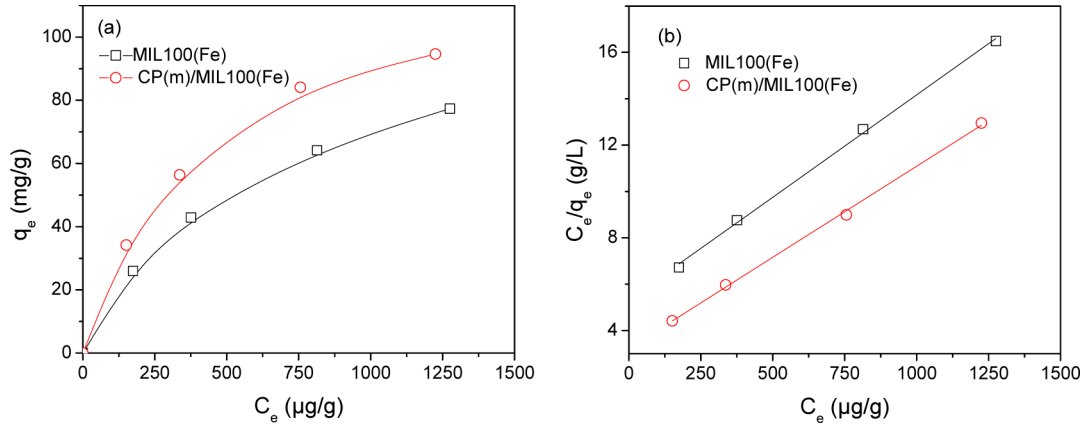

Figure 5. (a) The adsorption isotherms for BT and (b) Langmuir plots for the adsorptions over MIL100(Fe) and CP(m)/MIL100(Fe) at 25 °C.

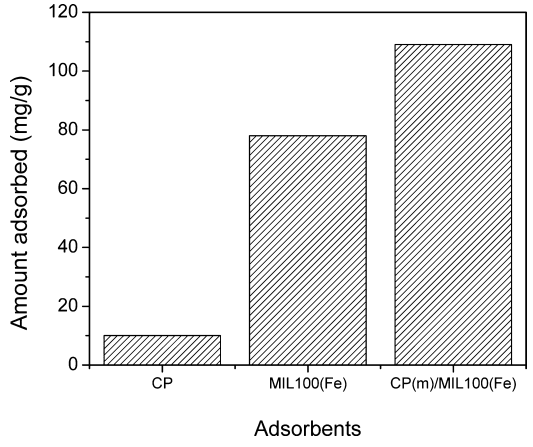

Figure 6. Adsorbed amounts of DBT over CP, MIL100(Fe), and CP(m)/MIL100(Fe). The adsorption time, temperature, and initial DBT concentration were 12 h, 25 °C, and 1000 μg/g, respectively.

4. CONCLUSION

The physicochemical properties of MOFs can be tuned by synthesizing composites through the dispersion of suitable materials with particular active sites. In this study, a stable Cu(I)-containing nonporous/nonsoluble CP (with a size much larger than the pore size of the MOFs) was successfully dispersed into MIL100(Fe) or CuBTC to prepare porous CP/MOF composites in a facile way. Both the dispersion of CP and the existence of Cu(I) were confirmed by TEM mapping and XPS studies, respectively. The composites have been used for the liquid-phase adsorption of BT or DBT from model fuel. The pseudo-second-order rate constant decreases as the CP content increases. This may be owed to the partial pore blocking which was also confirmed by the reduced pore sizes. Even with the reduced surface areas and pore volumes of the composite, the adsorption capacity for BT adsorption (based on both weight and the surface area of adsorbents) increased as the CP content increased, up to a certain value. This was probably as a result of the π-complexation between the well-dispersed Cu(I) and the BT or DBT. In summary, nonporous/nonsoluble MOFs (even with a relatively large crystal size compared to the cavity size of the porous MOFs) can be made composite with porous MOFs in a facile way. Accordingly, the dispersion of the nonporous MOFs can be highly enhanced, and this finally leads to the beneficial utilization of the active sites for adsorption.

■ ASSOCIATED CONTENT

Supporting Information

Preparation of MOFs, characterization of adsorbents, adsorption procedure, calculation of adsorption kinetics, calculation of maximum adsorption capacity (Q_0) and separation factor (R_L), XRD patterns of CuBTC and CP/CuBTC composites, SEM of

DOI: 10.1021/acsami.5b01642
ACS Appl. Mater. Interfaces 2015, 7, 10429−10435

CP and TEM-EDS mapping (CP(m)/MIL100(Fe), R_L values for adsorption of BT at different initial concentrations, and adsorption of BT over CP, CuBTC, and CP(m)/CuBTC. The Supporting Information is available free of charge on the ACS Publications website at DOI: 10.1021/acsami.5b01642.

AUTHOR INFORMATION

Corresponding Author

*Phone: 82-10-28185341. Fax: 82-53-950-6330. E-mail: sung@knu.ac.kr.

Present Address

†Department of Environment and Energy, Sejong University, Seoul 143-747, Republic of Korea.

Funding

This research was supported by the Basic Science Research Program through the National Research Foundation of Korea (NRF) grant funded by the Korea government (MSIP) (grant no. 2013R1A2A2A01007176).

Notes

The authors declare no competing financial interest.

REFERENCES

(1) Nakanishi, W.; Minami, K.; Shrestha, L. K.; Ji, Q.; Hill, J. P.; Ariga, K. Bioactive Nanocarbon Assemblies: Nanoarchitectonics and Applications. *Nano Today* **2014**, *9*, 378−394.

(2) Ariga, K.; Vinu, A.; Yamauchi, Y.; Ji, Q.; Hill, J. P. Nanoarchitectonics for Mesoporous Materials. *Bull. Chem. Soc. Jpn.* **2012**, *85*, 1−32.

(3) Ariga, K.; Ishihara, S.; Abe, H.; Lia, M.; Hill, J. P. Materials Nanoarchitectonics for Environmental Remediation and Sensing. *J. Mater. Chem.* **2012**, *22*, 2369−2377.

(4) Vinu, A.; Ariga, K. New Ideas for Mesoporous Materials. *Adv. Porous Mater.* **2013**, *1*, 63−71.

(5) Ariga, K.; Ito, H.; Hill, J. P.; Tsukube, H. Molecular Recognition: from Solution Science to Nano/Materials Technology. *Chem. Soc. Rev.* **2012**, *41*, 5800−5835.

(6) DeCoste, J. B.; Peterson, G. W. Metal−Organic Frameworks for Air Purification of Toxic Chemicals. *Chem. Rev.* **2014**, *114*, 5695−5727.

(7) Furukawa, H.; Cordova, K. E.; O'Keeffe, M.; Yaghi, O. M. The Chemistry and Applications of Metal-Organic Frameworks. *Science* **2013**, *341*, 1230444-12.

(8) Jhung, S. H.; Khan, N. A.; Hasan, Z. Analogous Porous Metal-Organic Frameworks: Synthesis, Stability and Application in Adsorption. *CrystEngComm* **2012**, *14*, 7099−7109.

(9) Voorde, B.V.de; Bueken, B.; Denayer, J.; De-Vos, D. Adsorptive Separation on Metal−Organic Frameworks in the Liquid Phase. *Chem. Soc. Rev.* **2014**, *43*, 5766−5788.

(10) Yang, Q.; Liu, D.; Zhong, C.; Li, J.-R. Development of Computational Methodologies for Metal−Organic Frameworks and Their Application in Gas Separations. *Chem. Rev.* **2013**, *113*, 8261−8323.

(11) Barea, E.; Montoro, C.; Navarro, J. A. R. Toxic Gas Removal Metal−Organic Frameworks for the Capture and Degradation of Toxic Gases and Vapours. *Chem. Soc. Rev.* **2014**, *43*, 5419−5430.

(12) Li, J.-R.; Sculley, J.; Zhou, H.-C. Metal-Organic Frameworks for Separations. *Chem. Rev.* **2012**, *112*, 869−932.

(13) Wu, H.; Gong, Q.; Olson, D. H.; Li, J. Commensurate Adsorption of Hydrocarbons and Alcohols in Microporous Metal-Organic Frameworks. *Chem. Rev.* **2012**, *112*, 836−868.

(14) Burtch, N. C.; Jasuja, H.; Walton, K. S. Water Stability and Adsorption in Metal−Organic Frameworks. *Chem. Rev.* **2014**, *114*, 10575−10612.

(15) Khan, N. A.; Hasan, Z.; Jhung, S. H. Adsorptive Removal of Hazardous Materials Using Metal-Organic Frameworks, (MOFs): a Review. *J. Hazard. Mater.* **2013**, *244−245*, 444−456.

(16) Hasan, Z.; Jhung, S. H. Removal of Hazardous Organics from Water Using Metal-Organic Frameworks (MOFs): Plausible Mechanisms for Selective Adsorptions. *J. Hazard. Mater.* **2015**, *283*, 329−339.

(17) Hasan, Z.; Tong, M.; Jung, B. K.; Ahmed, I.; Zhong, C.; Jhung, S. H. Adsorption of Pyridine over Amino-Functionalized Metal−Organic Frameworks: Attraction Via Hydrogen Bonding Versus Base−Base Repulsion. *J. Phys. Chem. C* **2014**, *118*, 21049−21056.

(18) Cohen, S. M. Postsynthetic Methods for the Functionalization of Metal−Organic Frameworks. *Chem. Rev.* **2012**, *112*, 970−1000.

(19) Goestena, M. G.; Juan-Alcañiz, J.; Ramos-Fernandez, E. V.; Gupta, K. B. S. S.; Stavitski, E.; Bekkum, H. V.; Gascon, J.; Kapteijn, F. Sulfation of Metal-Organic Frameworks: Opportunities for Acid Catalysis and Proton Conductivity. *J. Catal.* **2011**, *281*, 177−187.

(20) Hartmann, M.; Fischer, M. Amino-Functionalized Basic Catalysts with MIL-101 Structure. *Microporous Mesoporous Mater.* **2012**, *164*, 38−43.

(21) Thornton, A. W.; Nairn, K. M.; Hill, J. M.; Hill, A. J.; Hill, M. R. Metal-Organic Frameworks Impregnated with Magnesium-Decorated Fullerenes for Methane and Hydrogen Storage. *J. Am. Chem. Soc.* **2009**, *131*, 10662−10669.

(22) Khan, N. A.; Hasan, Z.; Jhung, S. H. Ionic Liquids Supported on Metal-Organic Frameworks: Remarkable Adsorbents for Adsorptive Desulfurization. *Chem.—Eur. J.* **2014**, *20*, 376−380.

(23) Zhu, Q.-L.; Xu, Q. Metal−Organic Framework Composites. *Chem. Soc. Rev.* **2014**, *43*, 5468−5512.

(24) Ahmed, I.; Jhung, S. H. Composites of Metal−Organic Frameworks: Preparation and Application in Adsorption. *Mater. Today* **2014**, *17*, 136−146.

(25) Li, Z.; Xiao, Y.; Xue, W.; Yang, Q.; Zhong, C. Ionic Liquid/Metal−Organic Framework Composites for H_2S Removal from Natural Gas: a Computational Exploration. *J. Phys. Chem. C* **2015**, *119*, 3674−3683.

(26) Levasseur, B.; Petit, C.; Bandosz, T. J. Reactive Adsorption of NO_2 on Copper-Based Metal−Organic Framework and Graphite Oxide/Metal−Organic Framework Composites. *ACS Appl. Mater. Interfaces* **2010**, *2*, 3606−3613.

(27) Liu, J.-W.; Zhang, Y.; Chen, X.-W.; Wang, J.-H. Graphene Oxide−Rare Earth Metal−Organic Framework Composites for the Selective Isolation of Hemoglobin. *ACS Appl. Mater. Interfaces* **2014**, *6*, 10196−10204.

(28) Du, D.-Y.; Qin, J.-S.; Li, S.-L.; Su, Z.-M.; Lan, Y.-Q. Recent Advances in Porous Polyoxometalate Based Metal−Organic Framework Materials. *Chem. Soc. Rev.* **2014**, *43*, 4615−4632.

(29) Doherty, C. M.; Knystautas, E.; Buso, D.; Villanova, L.; Konstas, K.; Hill, A. J.; Takahashi, M.; Falcaro, P. Magnetic Framework Composites for Polycyclic Aromatic Hydrocarbon Sequestration. *J. Mater. Chem.* **2012**, *22*, 11470−11474.

(30) Tanaka, K.; Muraoka, T.; Hirayama, D.; Ohnish, A. Highly Efficient Chromatographic Resolution of Sulfoxides Using a New Homochiral MOF−Silica Composite. *Chem. Commun.* **2012**, *48*, 8577−8579.

(31) Petit, C.; Bandosz, T. J. Engineering the Surface of a New Class of Adsorbents: Metal−Organic Framework/Graphite Oxide Composites. *J. Colloid Interface Sci.* **2015**, *447*, 139−151.

(32) Yang, S. J.; Choi, J. Y.; Chae, H. K.; Cho, J. H.; Nahm, K. S.; Park, C. R. Preparation and Enhanced Hydrostability and Hydrogen Storage Capacity of CNT@MOF-5 Hybrid Composite. *Chem. Mater.* **2009**, *21*, 1893−1897.

(33) Wang, X.; Wang, Q.; Wang, Q.; Gao, F.; Gao, F.; Yang, Y.; Guo, H. Highly Dispersible and Stable Copper Terephthalate Metal−Organic Framework−Graphene Oxide Nanocomposite for an Electrochemical Sensing Application. *ACS Appl. Mater. Interfaces* **2014**, *6*, 11573−11580.

(34) Juan-Alcañiz, J.; Gascon, J.; Kapteijn, F. Metal−Organic Frameworks as Scaffolds for the Encapsulation of Active Species: State of the Art and Future Perspectives. *J. Mater. Chem.* **2012**, *22*, 10102−10118.

DOI: 10.1021/acsami.5b01642
ACS Appl. Mater. Interfaces 2015, 7, 10429−10435

(35) Li, L.; Liu, X. L.; Gao, M.; Hong, W.; Liu, G. Z.; Fan, L.; Hu, B.; Xia, Q. H.; Liu, L.; Song, G. W.; Xu, Z. S. The Adsorption on Magnetic Hybrid Fe_3O_4/HKUST-1/GO of Methylene Blue from Water Solution. *J. Mater. Chem. A* **2014**, *2*, 1795−1801.
(36) Sun, C.-Y.; Liu, S.-X.; Liang, D.-D.; Shao, K.-Z.; Ren, Y.-H.; Su, Z.-M. Highly Stable Crystalline Catalysts Based on a Microporous Metal-Organic Framework and Polyoxometalates. *J. Am. Chem. Soc.* **2009**, *131*, 1883−1888.
(37) Song, J.; Luo, Z.; DBritt, K.; Furukawa, H.; Yaghi, O. M.; Hardcastle, K. I.; Hill, C. L. A Multiunit Catalyst with Synergistic Stability and Reactivity: A Polyoxometalate Metal Organic Framework for Aerobic Decontamination. *J. Am. Chem. Soc.* **2011**, *133*, 16839−16846.
(38) Khan, N. A.; Jhung, S. H. Adsorptive Removal of Benzothiophene Using Porous Copper-Benzenetricarboxylate Loaded with Phosphotungstic Acid. *Fuel Process. Technol.* **2012**, *100*, 49−54.
(39) Samokhvalov, A.; Tatarchuk, B. J. Review of Experimental Characterization of Active Sites and Determination of Molecular Mechanisms of Adsorption, Desorption and Regeneration of the Deep and Ultradeep Desulfurization Sorbents for Liquid Fuels. *Catal. Rev. Sci. Eng.* **2010**, *52*, 381−410.
(40) Stanislaus, A.; Marafi, A.; Rana, M. S. Recent Advances in the Science and Technology of Ultra Low Sulfur Diesel (ULSD) Production. *Catal. Today* **2010**, *153*, 1−68.
(41) Hasan, Z.; Jeon, J.; Jhung, S. H. Oxidative Desulfurization of Benzothiophene and Thiophene with WO_x/ZrO_2, Catalysts: Effect of Calcination Temperature of Catalysts. *J. Hazard. Mater.* **2012**, *205−206*, 216−221.
(42) Yang, R. T.; Hernandez-Maldonaldo, A. J.; Yang, F. H. Desulfurization of Transportation Fuels with Zeolites under Ambient Conditions. *Science* **2003**, *301*, 79−81.
(43) Hernández-Maldonad, A. J.; Yang, R. T. Desulfurization of Diesel Fuels by Adsorption via Pi-Complexation with Vapor-Phase Exchanged Cu(I)-Y Zeolites. *J. Am. Chem. Soc.* **2004**, *126*, 992−993.
(44) Wang, Y.; Yang, R. T. Desulfurization of Jet Fuel JP-5 Light Fraction by MCM-41 and SBA-15 Supported Cuprous Oxide for Fuel Cell Applications. *Ind. Eng. Chem. Res.* **2009**, *48*, 142−147.
(45) Yang, X.; Erickson, L. E.; Hohn, K. L. Sol−Gel Cu-Al_2O_3 Adsorbents for Selective Adsorption of Thiophene out of Hydrocarbon. *Ind. Eng. Chem. Res.* **2006**, *45*, 6169−6174.
(46) Khan, N. A.; Jhung, S. H. Remarkable Adsorption Capacity of $CuCl_2$-Loaded Porous Vanadium Benzenedicarboxylate for Benzothiophene. *Angew. Chem., Int. Ed.* **2012**, *51*, 1198−1201.
(47) Khan, N. A.; Jhung, S. H. Low-temperature Loading of Cu^+ Species over Porous Metal-Organic Frameworks (MOFs) and Adsorptive Desulfurization with Cu^+-loaded MOFs. *J. Hazard. Mater.* **2012**, *237−238*, 180−185.
(48) Ahmed, I.; Jhung, S. H. Adsorptive Denitrogenation of Model Fuel with CuCl-Loaded Metal−Organic Frameworks (MOFs). *Chem. Eng. J.* **2014**, *251*, 35−42.
(49) Mohapatra, S.; Maji, T. K. Facile Synthesis of Anion Dependent Versatile Cu^I and Mixed-Valent Porous Cu^I/Cu^{II} Frameworks. *Dalton Trans.* **2010**, *39*, 3412−3419.
(50) Maji, T. K.; Ghoshal, D.; Zangrando, E.; Ribas, J.; Chaudhuri, N. R. A Novel 2D Mixed Valence Copper (I/II) Rectangular Grid Constructed with Pyrazine and Croconate. *CrystEngComm* **2004**, *6*, 623−626.
(51) Zhang, J.-P.; Kitagawa, S. Supramolecular Isomerism, Framework Flexibility, Unsaturated Metal Center, and Porous Property of Ag(I)/Cu(I) 3,3′,5,5′-Tetrametyl-4,4′-Bipyrazolate. *J. Am. Chem. Soc.* **2008**, *130*, 907−917.
(52) Lu, J. Y. Crystal Engineering of Cu-containing Metal−Organic Coordination Polymers under Hydrothermal Conditions. *Coord. Chem. Rev.* **2003**, *246*, 327−347.
(53) Amo-Ochoa, P.; Givaja, G.; Miguel, P. J. S.; Castillo, O.; Zamora, F. Microwave Assisted Hydrothermal Synthesis of a Novel CuI-sulfate-pyrazine MOF. *Inorg. Chem. Commun.* **2007**, *10*, 921−924.
(54) Horcajada, P.; Surblé, S.; Serre, C.; Hong, D.-Y.; Seo, Y.-K.; Chang, J.-S.; Grenèche, J.-M.; Margiolakid, I.; Férey, G. Synthesis and Catalytic Properties of MIL-100 (Fe), an Iron(III) Carboxylate with Large Pores. *Chem. Commun.* **2007**, *27*, 2820−2822.
(55) Chui, S. S.-Y.; Lo, S. M. -F.; Charmant, J. P. H.; Orpen, A. G.; Williams, I. D. A. Chemically Functionalizable Nanoporous Material $[Cu_3(TMA)_2(H_2O)_3]$n. *Science* **1999**, *283*, 1148−1150.
(56) Seo, Y.-K.; Yoon, J. W.; Lee, J. S.; Lee, U.-H.; Hwang, Y. K.; Jun, C.-H.; Horcajada, P.; Serre, C.; Chang, J.-S. Large Scale Fluorine-Free Synthesis of Hierarchically Porous Iron(III) Trimesate MIL-100(Fe) with a Zeolite MTN Topology. *Microporous Mesoporous Mater.* **2012**, *157*, 137−145.
(57) Khan, N. A.; Enamul, H.; Jhung, S. H. Rapid syntheses of A Metal−Organic Framework Material $Cu_3(BTC)_2(H_2O)_3$ under Microwave: a Quantitative Analysis of Accelerated Syntheses. *Phys. Chem. Chem. Phys.* **2010**, *12*, 2625−2631.
(58) Singh, K. P.; Mohan, D.; Sinha, S.; Tondon, G. S. Color Removal from Wastewater Using Low-Cost Activated Carbon Derived from Agricultural Waste Material. *Ind. Eng. Chem. Res.* **2003**, *42*, 1965−1976.
(59) Önal, Y.; Akmil-Başar, C.; Sarıcı-Özdemir, Ç. Elucidation of the Naproxen Sodium Adsorption onto Activated Carbon Prepared from Waste Apricot: Kinetic, Equilibrium and Thermodynamic Characterization. *J. Hazard. Mater.* **2007**, *148*, 727−734.
(60) Ho, Y.-S.; Chiang, T.-H.; Hsueh, Y.-M. Removal of Basic Dye from Aqueous Solution Using Tree Fern as a Biosorbent. *Process Biochem.* **2005**, *40*, 119−124.
(61) Belhachemi, M.; Addoun, F. Comparative Adsorption Isotherms and Modeling of Methylene Blue onto Activated Carbons. *Appl. Water Sci.* **2011**, *1*, 111−117.
(62) Khan, N. A.; Hasan, Z.; Min, K. S.; Paek, S. M.; Jhung, S. H. Facile Introduction of Cu^+ on Activated Carbon at Ambient Conditions and Adsorption of Benzothiophene over Cu^+ /Activated Carbon. *Fuel Process. Technol.* **2013**, *116*, 265−270.
(63) Song, X.-L.; Sun, L.-B.; He, G.-S.; Liu, X.-Q. Isolated Cu(I) Sites Supported on β-Cyclodextrin: An Efficient π-Complexation Adsorbent for Thiophene Capture. *Chem. Commun.* **2011**, *47*, 650−652.
(64) Jiang, W.-J.; Yin, Y.; Liu, X.-Q.; Yin, X.-Q.; Shi, Y.-Q.; Sun, L.-B. Fabrication of Supported Cuprous Sites at Low Temperatures: An Efficient, Controllable Strategy Using Vapor-Induced Reduction. *J. Am. Chem. Soc.* **2013**, *135*, 8137−8140.
(65) He, G.-S.; Sun, L.-B.; Song, X.-L.; Liu, X.-Q.; Yin, Y.; Wang, Y.-C. Adjusting Host Properties to Promote Cuprous Chloride Dispersion and Adsorptive Desulfurization Sites Formation on SBA-15. *Energy Fuels* **2011**, *25*, 3506−3513.
(66) Yin, Y.; Jiang, W.-J.; Liu, X.-Q.; Li, Y.-H.; Sun, L.-B. Dispersion of Copper Species in a Confined Space and Their Application in Thiophene Capture. *J. Mater. Chem.* **2012**, *22*, 18514−18521.
(67) Yang, Q.; Zhong, C. Molecular Simulation of Carbon Dioxide/Methane/Hydrogen Mixture Adsorption in Metal−Organic Frameworks. *J. Phys. Chem. B* **2006**, *110*, 17776−17783.
(68) Khan, N. A.; Hasan, Z.; Jhung, S. H. Adsorption and Removal of Sulfur or Nitrogen-containing Compounds with Metal−Organic Frameworks (MOFs): A Review. *Adv. Porous Mater.* **2013**, *1*, 91−102.

DOI: 10.1021/acsami.5b01642
ACS Appl. Mater. Interfaces 2015, 7, 10429−10435